Philips Res. Repts 32, 436-459, 1977

INTERMODULATION AND MOIRÉ EFFECTS IN OPTICAL VIDEO RECORDING

by M. R. DE HAAN and C. H. F. VELZEL

Abstract

In optical video disc recording there are several nonlinear operations that generate intermodulation products between the luminance, chrominance and audio components of the recorded signals. The different processing steps are: modulation, laser-beam writing, disc fabrication, laser-beam reading and demodulation. We give mathematical models for each of these steps and calculate the mixing products for the case of a NTSC direct FM system, as chosen for the optical disc system proposed by Philips and MCA.

1. Introduction

1.1. *The video disc system* (see also refs 1–4)

A video disc system for domestic applications must be able to store about 30 minutes of a colour video signal and sound signals in the tracks of a disc 30 cm in diameter. As the linear recording density in an optical system can be chosen in the order of 1000 periods per mm, this allows the choice of the attractive recording format of exactly one television frame per revolution. By jumping synchronously between tracks it thus becomes possible to select other display modes like stop frame, fast forward or reverse motion. The track density in radial direction can be 600 tracks per mm. The tracks are spirally aligned.

1.2. *The recording and reading process*

All the necessary signals — at least luminance, chrominance and sound — have to be combined into one writing signal suitable for driving an electro-optical or acousto-optical light-modulator. In general this writing signal will have a square-wave form (see fig. 1) that will switch a writing laser beam on and off, which is focused on the photoresist surface of the rotating master disc. After development pits will be created in the photoresist layer at the exposed

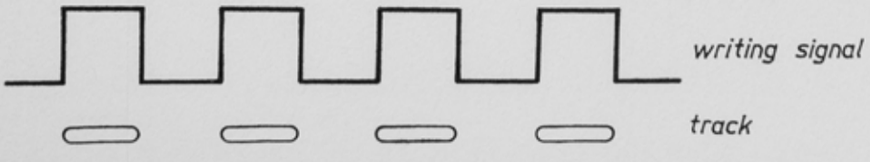

Fig. 1. The writing signal that drives the laser-beam modulator and the resulting track.

areas [1]). Replicas from the master disc can be produced by means of various processing techniques (fig. 2). The written tracks can be read again by means of a reading laser beam held in focus and correctly positioned upon the track by appropriate servo systems [2]).

In both writing and reading the bandwidth-restricting element is found by the combination of the finite spot size and the tangential velocity of the track with respect to the write/read beam. The numerical aperture N of the objective used and the wavelength λ of the laser beam define the modulation transfer function with which a grating-like structure can be read or written. The absolute cut-off periodicity p_c is given by

$$p_c = \lambda/2N. \tag{1}$$

The relationship between the spatial frequency $1/p$ and the frequency ω of the electrical signal is given by

$$\omega = 4\,\pi^2\, R f_r/p \tag{2}$$

where R is the radius of the track, and f_r is the revolution frequency of the disc.

Having chosen a fixed revolution frequency $f_r = 30$ Hz the amplitude versus frequency characteristic will be clearly dependent on the radius. In figure 3 the

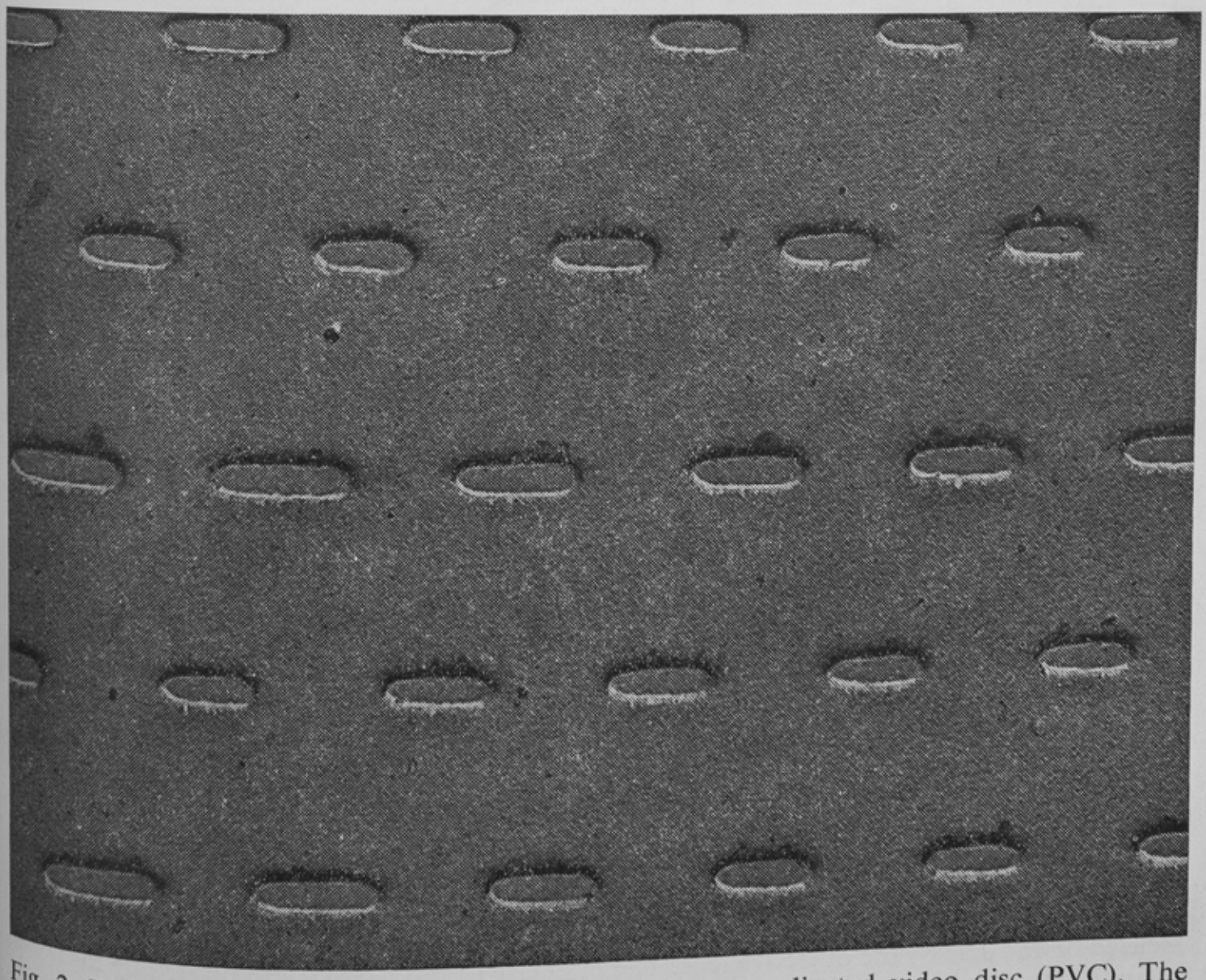

Fig. 2. Electron microscope picture of the tracks on a replicated video disc (PVC). The distance between the tracks is about 2 μm.

characteristic of the playback system is given for two radii and corresponds to a numerical aperture of 0.40 and a wavelength $\lambda = 633$ nm. For recording a shorter wavelength and a higher numerical aperture is used. For example with $\lambda = 458$ nm and $N = 0.72$ the writing amplitude characteristic is expanded by a factor 2.5 on the frequency axis with respect to fig. 3.

In the transmission channel a number of nonlinear operations occur (see fig. 4). The first element, generating the square-wave writing signal, is in general an electronic hard limiter whether it is used as part of a pulsewidth modulator or as the last stage of a FM modulator for the luminance signal. We will see in the subsequent sections how an asymmetrical setting of the limiter level, result-

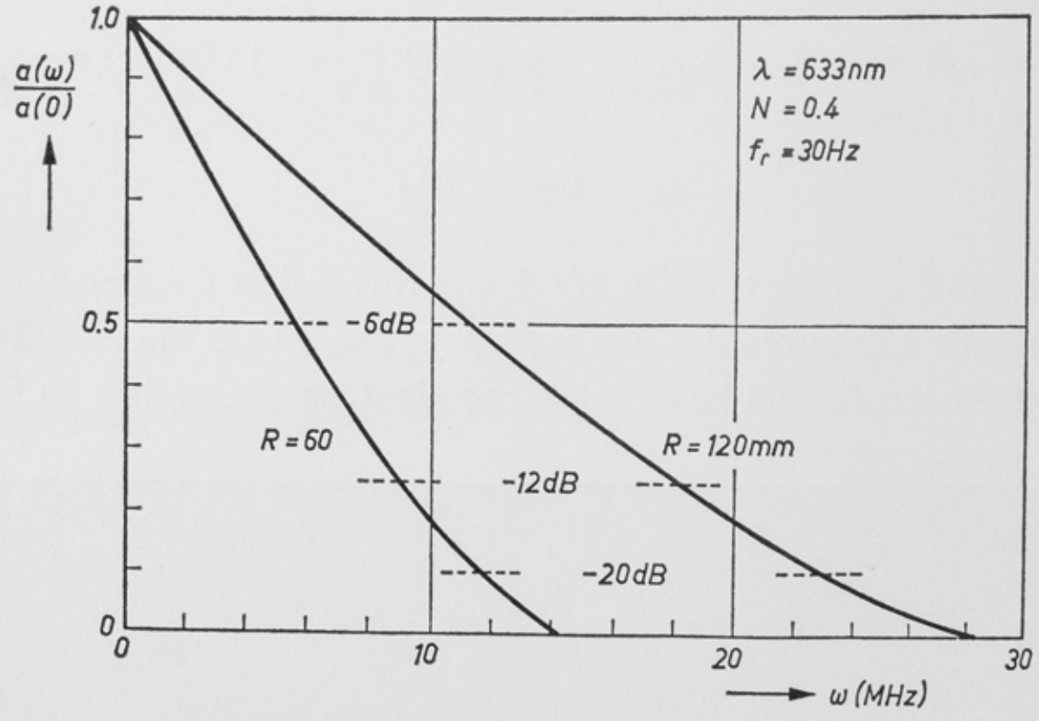

Fig. 3. Amplitude versus frequency characteristic of the photodetector signal, corresponding to a numerical aperture 0.4 of the reading objective and a 30 Hz revolution frequency of the disc.

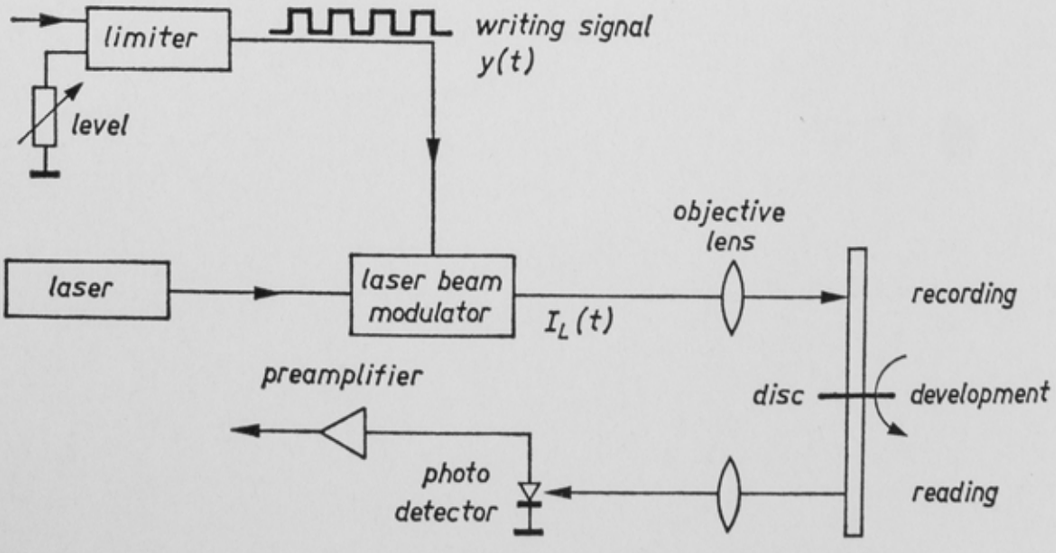

Fig. 4. Schematic diagram of the mastering process. The output beam of the writing laser is focused on the disc by the objective lens. The intensity of the beam is modulated by the signal of fig. 7. The disc is covered by photoresist, rotates at 30 Hz and moves relative to the writing beam at a speed of about 50 μm per second in the radial direction.

ing in a non-zero time average of the writing signal $y(t)$ can affect the generation of intermodulation components from different source frequencies. The electro-optical modulator has a raised cosine-function characteristic between input drive voltage and output light intensity. Normally the soft nonlinearity of such a characteristic is completely overruled by the hard-limiter nonlinearity so that in a good approximation we can forget the EO modulator except for the setting of its working point that has the same effect as the symmetry-setting of the electronic limiter.

Further nonlinearities are present in the writing and development steps. Here the length of the written pits may be shorter or longer than originally intended, due to the influence of the writing laser intensity, the sensitivity of the photoresist and its development time. Also additional variations may occur in pit dimensions during the replication process.

This inherent asymmetry of the recording process represents one of the major differences with respect to magnetic recording, where only the direction of magnetization is altered. The effect of this symmetry distortion on the signal read during playback can under some circumstances be represented as an offset shift of the symmetry setting of the hard limiter. Finally the reading mechanism itself introduces a nonlinearity, basically because we read a squared signal due to the fact that the photodetector is only sensitive to the intensity of reflected light and not to its amplitude.

1.3. *Signal encoding*

Two basic approaches for the encoding of a composite video signal are possible, assuming that it is desirable to maintain the chrominance information in its quadrature-modulated format. The first method consists of separation of the chrominance subcarrier from the luminance part and encoding them differently, for example in a "colour under" or "crossband" scheme [6]), where the subcarrier is transposed to a lower frequency. These systems are mostly used where the recording medium has a rather limited bandwidth. Separation of luminance and chrominance always causes additional signal degradation and restricts the luminance bandwidth [3]). The second method is a direct one, where the composite video signal is transmitted as such through the system. If the medium has sufficient bandwidth the direct method is to be preferred as it maintains the full luminance and chroma bandwidth [4]). For the purpose of this paper we will only refer to a direct system that uses the NTSC standard.

In designing the encoding system it is apparent that one has to consider the amplitude characteristic corresponding to the smallest radius to be read. In contrast to the draw-back of a varying amplitude characteristic as a function of radius, we have the advantage of a constant group delay as a function of frequency and radius. Besides the slow changes in amplitude with radius, fast variations can occur due to instantaneous deviations from the correct focus or

to radial tracking errors. Hence, as in magnetic recording, frequency modulation is most appropriate for recording the video signal. Considering figure 3 it appears that usable carrier frequencies can be chosen up to 10 MHz depending on the innermost radius chosen. As we will see in the following sections, the specific choice of carrier frequencies is closely related to the positions of the most important intermodulation components on the frequency axis.

In our case the composite video signal is applied to the input of an FM modulator with a black-to-white frequency deviation from 8.0 MHz to 9.2 MHz. Sync tip is at 7.5 MHz. The spectrum of the output signal of the FM modulator, having a sinusoidal or triangular-wave form, is shown in fig. 5 only for the main carrier and two first-order sidebands of the colour subcarrier at distances of 3.58 MHz. The positions of these colour sidebands follow the motion of the main carrier on the frequency axis depending on the instantaneous luminance level to be recorded. For a continuous fixed grey level superimposed with a continuous subcarrier the spectrum would only consist of three unmodulated frequencies, disregarding the second and higher-order sidebands, at 8.60 and 8.60 ± 3.58 MHz.

The pre-emphasis, normally used in a FM channel to reduce the effect of triangular noise [10]) at the higher video frequencies, is so chosen in our case as to give a relative amplification $a_c = 2$ at the subcarrier frequency ω_c ($\tau_1 = 125$ ns, $\tau_r = 50$ ns).

Therefore, the resulting modulation index for the chrominance sidebands is given by

$$m = \frac{a_c \, \Delta\omega}{\omega_c} \frac{V_C}{V_{BW}}, \tag{3}$$

where $2\Delta\omega$ is the black-to-white deviation (1.2 MHz),

V_C the peak-peak amplitude of the chrominance and

V_{BW} the black-to-white amplitude of the luminance signal, normally equal to 700 mV.

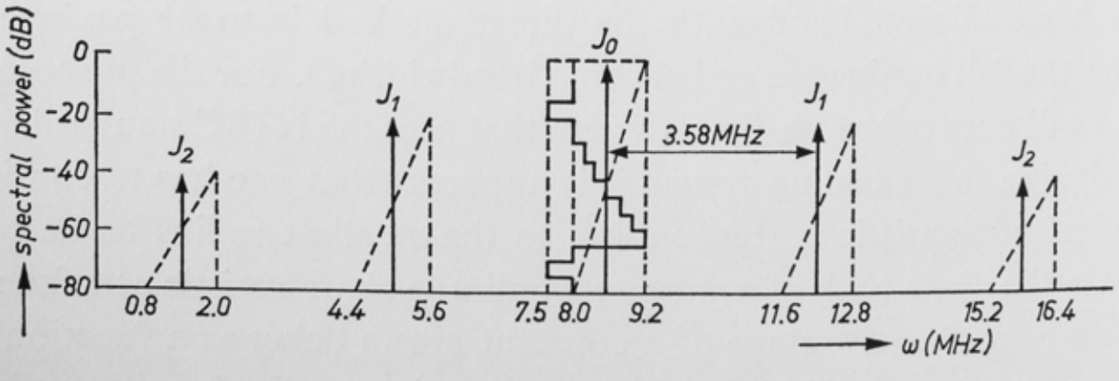

Fig. 5. Spectrum of the frequency-modulated composite video signal (NTSC). Black-to-white deviation from 8.0 to 9.2 MHz. Pre-emphasis constants $\tau_1 = 125$ ns, $\tau_2 = 50$ ns.

For $V_C = 675$ mV we have $m = 0.32$ and $J_1(m) = 0.16$ (−16 dB), $J_2(m) = -38$ dB, and $J_3(m) = -63$ dB. $V_C = 675$ mV corresponds to 75% saturated cyanic or red colours. The two sound channels are located at 2.3 and 2.8 MHz respectively and consist of FM-modulated subcarriers. As shown in fig. 6 these signals are linearly added to the output of the video FM modulator and then applied to a limiter. This operation results in a pulsewidth modulation as indicated for one subcarrier in fig. 7.

The complete spectrum of the recording signal before limiting is now given in fig. 8. The amplitudes of the sound carriers are chosen at −20 dB compared to the main carrier. After limiting, their amplitude is reduced by a factor of 2, resulting in a level of −26 dB compared to the main carrier. It is of interest now

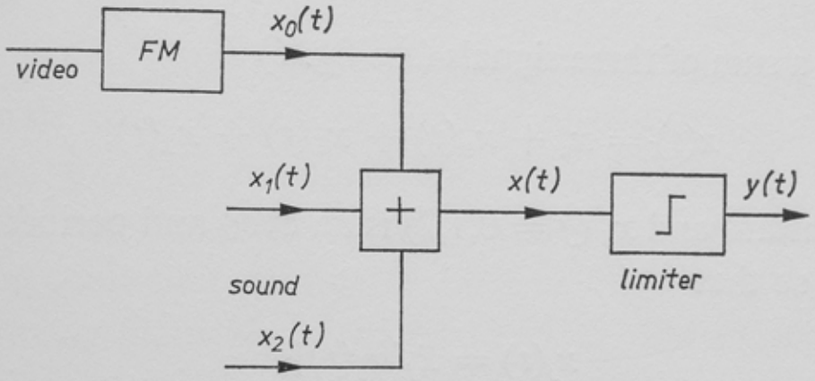

Fig. 6. Generation of the modulator signal. The luminance carrier, FM-modulated by the video signal, is added to the sound signals. The sum signal is limited, so that a duty cycle and frequency-modulated block signal results.

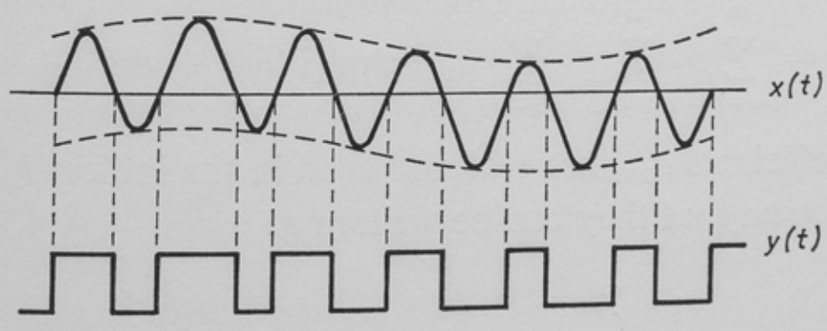

Fig. 7. Principle of pulsewidth modulation; $x(t)$ is input signal to the limiter, $y(t)$ is the resulting output signal.

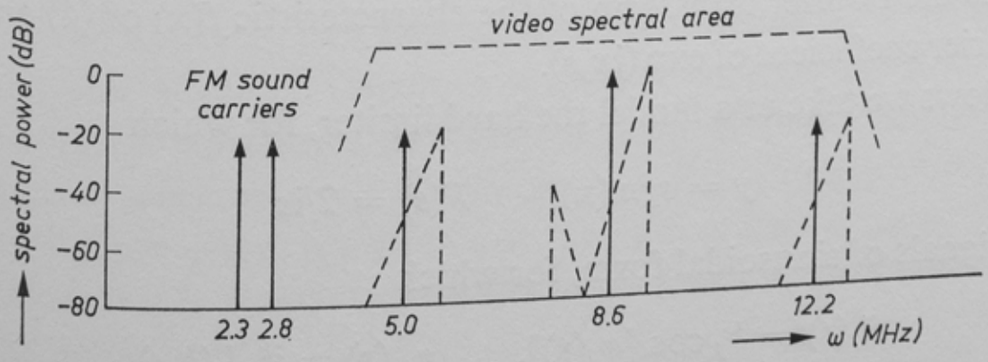

Fig. 8. Spectrum of the signal $x(t)$, consisting of the addition of two sound carriers to the output signal of the FM modulator for the video signal.

to investigate in more detail the effects of nonlinear steps on this input spectrum. We will see how the positions and amplitudes of intermodulation products are derived, and how some components depend strongly on the symmetry setting of the nonlinearities, starting with the electronic limiter.

2. Intermodulation products of a memoryless limiter

The first element in the signal-processing chain of the VLP system shown in fig. 4 is a limiter. We will assume that the bandwidth of this device is large compared to that of subsequent stages, so that we can consider it as a memoryless device. With an output $y(t)$ and an input $x(t)$, let the characteristic of this device be given by

$$y = f(x). \tag{4}$$

Let the input be a sum of three signals (see fig. 6)

$$x(t) = x_a + x_0(t) + x_1(t) + x_2(t), \tag{5}$$

where x_a is a constant and x_j ($j = 0,1,2$) is an even and periodic function of an argument $\varphi_j(t)$, so that

$$x_j(t) = \tilde{x}_j[\varphi_j(t)]$$

and

$$\tilde{x}_j(\varphi_j) = \tilde{x}_j(\varphi_j + 2\pi) = \tilde{x}_j(-\varphi_j). \tag{6}$$

The output $y(t)$ can now be written as a triple Fourier series:

$$y = \sum_{l=-\infty}^{\infty} \sum_{m=-\infty}^{\infty} \sum_{n=-\infty}^{\infty} a_{lmn} \exp\left[\mathrm{i}\,(l\varphi_0 + m\varphi_1 + n\varphi_2)\right] \tag{7}$$

of which the coefficients a_{lmn} are real and even in the indices l, m and n. In the appendix it is shown that they can be written as

$$a_{lmn} = \frac{1}{2\pi} \int_{-\infty}^{\infty} F(s) \exp(\mathrm{i}x_a s)\, g_{0l}(s)\, g_{1m}(s)\, g_{2n}(s)\, \mathrm{d}s, \tag{8}$$

where $F(s)$ is the Fourier transform of the characteristic $f(x)$ of (4) and $g_{jk}(s)$ is the kth Fourier coefficient of $\exp(\mathrm{i}x_j s)$.
In what follows we take as a model the hard limiter, for which

$$y = sgn\,(x), \qquad F(s) = 2/\mathrm{i}s \tag{9}$$

and input signals of sinusoidal form, for which

$$\tilde{x}_j(t) = b_j \cos\left[\varphi_j(t)\right], \qquad g_{jk}(s) = \mathrm{i}^k J_k(b_j s), \tag{10}$$

where $J_k(z)$ is the Bessel function of the first kind, of order k, argument z (ref. 8). Because the parity of $J_k(z)$ is that of its order, it follows from (8), (9) and (10)

that for a hard limiter with sinusoidal inputs

$$a_{lmn} = \frac{(-1)^{(l+m+n)/2}}{\pi} \int_{-\infty}^{\infty} \frac{\sin(x_a s)}{s} J_l(b_0 s)\, J_m(b_1 s)\, J_n(b_2 s)\, \mathrm{d}s \qquad (11)$$

when $l + m + n$ is even, and that

$$a_{lmn} = \frac{(-1)^{(l+m+n)/2}}{\pi} \int_{-\infty}^{\infty} \frac{\cos(x_a s)}{s} J_l(b_0 s)\, J_m(b_1 s)\, J_n(b_2 s)\, \mathrm{d}s \qquad (12)$$

when $l + m + n$ is uneven. It is seen from (11) and (12) that for $x_a \to 0$ the coefficients of even order are proportional to x_a and the coefficients of uneven order are independent of x_a. It should be noted that φ_j in (6) need not be linear in t. Any single-valued continuous function of t can be inserted, so that phase-modulated signals can be also taken into consideration. We will use this property in sec. 4.2. We presented the discussion of the intermodulation products of the limiter in this section, because it is the first element of the signal-processing chain and dominates the generation of modulation products. In fact we will make plausible in the next section that an asymmetric limiting process ($x_a \neq 0$), followed by a linear filter, is a reasonably good approximation for signal processing in the VLP system.

3. A mathematical model of recording and playback

In this section we develop a mathematical model for the signal processing of the VLP system shown in fig. 4. The output signal $y(t)$ of the limiter drives the modulator. When we assume a hard-limiter characteristic (eq. (8)) the intensity of the writing laser beam is proportional to $y(t)$. The exposure pattern on the master disc (for a description of the mastering process see ref. 1) is now given by

$$E(u,v) = I_L \int y(t)\, A(u - \mathrm{st}, v)\, \mathrm{d}t, \qquad (13)$$

where I_L is the power of the writing laser, u and v are tangential and radial coordinates in the plane of the disc (see ref. 9) and $A(u,v)$ is the point spread function of the objective lens that is used for focusing the laser beam on the master disc. The tangential velocity s of the disc depends on the track radius [1]. By processing of the master disc and pressing of plastic replicas the video recording process is completed [1]. We obtain a disc with depressions (see fig. 2) whose phase depth $\varphi(u,v)$ is a nonlinear function of the exposure.

In reference 9 it is shown that as the input signal of the player can be considered the quantity

$$S(u) = \int_{-\gamma/2+v_0}^{\gamma/2+v_0} [\exp \mathrm{i}\varphi(u,v) - 1]\, \mathrm{d}v, \qquad (14)$$

where γ is the width of a track so that the domain of integration is a track of the information pattern at a radial distance v_0 from the optical axis. We see from (13) and (14) that the signal $S(u)$, that is proportional to γ, for a track of uniform cross-section, is formed from $y(t)$ by a rather intricate nonlinear process. We approximate this process by a linear filter (the writing spot) followed by a memoryless nonlinearity. As a simple model of this nonlinearity we take a power characteristic, so that

$$S(u) = a\,[I_L \int y(t)\, A(u - st, v_0)\, \mathrm{d}t]^{\Gamma}, \tag{15}$$

where a is a complex constant, and $A(u,v_0)$ is our approximation of the linear filter. The exponent Γ can be compared to the gamma of a photographic recording. Because $y(t)$ is a two-level signal with an average frequency that is low compared to the cut-off frequency of the filter, this is an adequate approximation. In reference 9 it is also shown that the output signal of the playback unit is given by

$$\begin{aligned} i(t) = I_0\,[1 + 2\,\mathrm{Re} \int H(u)\, S(u - st)\, \mathrm{d}u + \\ + \int\int G(u,u')\, S(u - st)\, S^*(u' - st)\, \mathrm{d}u\, \mathrm{d}u'\,], \end{aligned} \tag{16}$$

which is a bilinear functional of $S(u)$, where S^* is the complex conjugate of S; $i(t)$ is a function of time because the information pattern $S(u)$ moves along the reading spot with a tangential velocity s, in principle the same as in the recording process (real time recording, see ref. 1). The constant I_0 in (16) is proportional to the power of the reading laser, $H(u)$ is a linear point spread function proportional to the intensity distribution of the reading spot along the track. $G(u,u')$ is a two-dimensional point spread function defined in ref. 9. It is seen that the third term of $i(t)$ contains the sum and difference frequencies of the harmonics of $S(u)$. This is to be expected from the quadratic character of the detection mechanism.

The two equations (15) and (16) form our mathematical model of the recording and reading processes. Equation (15) is less exact than (16), but the bandwidth of the filter $A(u-st, v_0)$ of the writing process is much larger than that of the filters $H(u)$ and $G(u,u')$ of the playback unit, so that the influence of the recording process after the limiter, which is at the beginning of the chain, is not so important. We now consider the modulation products of both parts of the system.

3.1. *Intermodulation in the recording process*

When the linear filter provided by the writing spot has a large bandwidth, the processing from the limiter of a frequency-modulated block signal $y(t)$ can be described as a distortion of the flanks of the pulses, as is shown in fig. 9. It is seen in fig. 9 that the chief effect of this distortion is that, for the chosen value

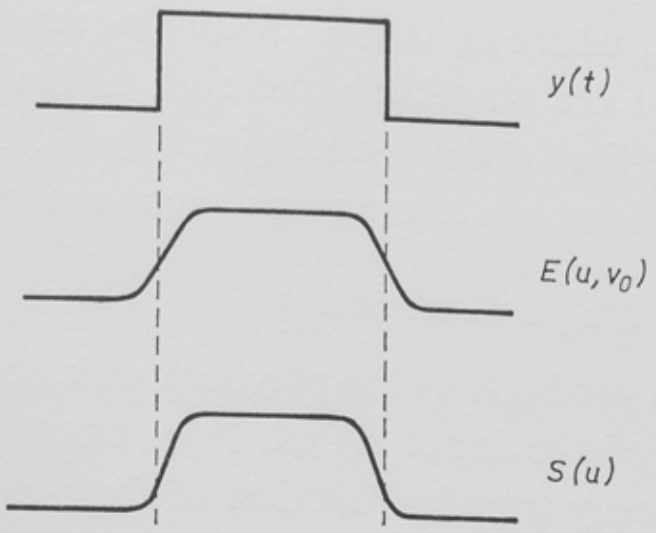

Fig. 9. Signal processing by recording and development; $y(t)$ is the input signal, the intensity of the laser beam is proportional to it; $E(u,v_0)$ results by linear filtering of $y(t)$, it is the exposure in the middle of the track; $S(u)$ results by distortion of $E(u,v_0)$, it is proportional to the track width and serves as an input signal to the playback unit.

of $\Gamma = 2$, the pulses become somewhat shorter. It is also possible, by controlling the intensity of the writing beam and the development time of the master, to change Γ considerably and obtain longer pulses. The influence on the final pit length of both these parameters is predominant.

Shortening or lenghtening of the pits by a fixed amount can be also achieved, with a signal of fixed frequency, by asymmetric limiting ($x_a \neq 0$ in (5). But for a frequency-modulated signal the two methods are not equivalent. Asymmetric limiting by a memoryless device gives only higher-order signals, whereas a device with memory, such as (15), can also give rise to baseband components. In figure 10 we give the first-order components of a frequency-modulated $y(t)$ with carrier frequency ω_0 and modulation index m. The sidebands, that have opposite sign, lie at distances $\pm\,\omega_c$ from the carrier. Filtering by means of the writing spot weakens the upper sideband somewhat relative to the lower sideband. The filtered spectrum can be written as the sum of a frequency-modulated signal and a sinusoidal signal at the frequency $\omega_0 + \omega_c$. A quadratic nonlinearity gives a mixing product at the frequency ω_c, called a baseband component. Relative to that of the carrier ω_0, the approximate amplitude of this

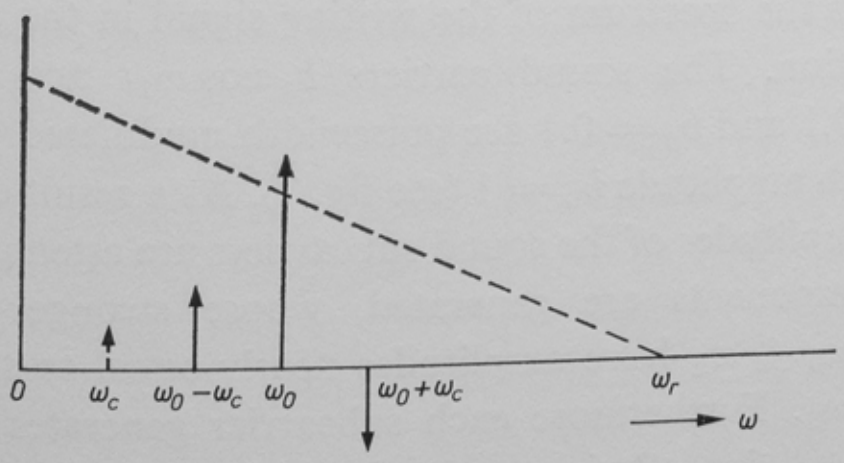

Fig. 10. First-order components of the FM signal at ω_0 and $\omega_0 \pm \omega_c$; baseband component at ω_c. The modulation transfer of the recording process, with cut-off frequency at ω_r, is shown as a broken line.

component is $2m\omega_0/\omega_r$, where ω_r is the cut-off frequency of the filter of (15). It should be noted that the amplitude and sign of the baseband component follow from the properties of the model given by (15). That means that by controlling carefully the process these parameters can be changed.

3.2. *Intermodulation in the playback unit*

The intermodulation products of the playback unit consists of the sum- and difference frequencies of the input signal. Approximate expressions for the two-dimensional frequency transfer function of the player are given in ref. 9. When the amplitudes of the components at ω_c generated by mixing ω_0 with $\omega_0 \pm \omega_c$ are different we obtain a baseband component.

Because the third term in (16) is quadratic, the amplitude of the baseband component is proportional to $2m\omega_c/\omega_p$, where ω_p is the cut-off frequency of the playback unit. In practice the cut-off frequency ω_p of the playback unit is much smaller than the cut-off frequency ω_r of the recording process.

As both the recording and the reading process generate baseband components it is in principle possible to compensate the two with each other so that the amplitude of the baseband component in $i(t)$ becomes zero. This requires, however, a very accurate technology [1]).

We will next approximate the total system by an asymmetric limiter, followed by a linear filter with cut-off frequency ω_p. From the above it will be clear that this is a rather rough approximation. With the aid of the more precise models given in refs 1 and 9 the approximation may be improved considerably.

4. Intermodulation components for a direct NTSC system

In this section we will deal successively with the intermodulation products between luminance and sound carriers, between luminance and colour sidebands and between sound and colour sidebands.

4.1. *Luminance and sound*

Figure 11 shows the spectrum of the writing signal in the absence of chrominance information. The sound carriers $b_1 \cos \omega_1 t$ and $b_2 \cos \omega_2 t$ with amplitudes $b_1 = 0.1$ and $b_2 = 0.1$ are pulsewidth modulated on the main carrier $b_0 \cos \omega_0 t$ with amplitude $b_0 = 1$ (see fig. 7). As a result of the pulsewidth modulation the amplitudes of the sound subcarriers are attenuated by 6 dB and new spectral components are generated, whose stronger components at $2\omega_0 \pm \omega_1$ and $2\omega_0 \pm \omega_2$ have amplitudes nearly equal to those of the subcarriers ω_1 and ω_2. Furthermore each subcarrier generates the components $\omega_0 \pm 2\omega_1$ and $\omega_0 \pm 2\omega_2$. Owing to the fact that two subcarriers are present we also get significant cross components at $\omega_0 \pm \omega_1 \pm \omega_2$. The movement of the instantaneous carrier frequency ω_0 as a function of the luminance level of

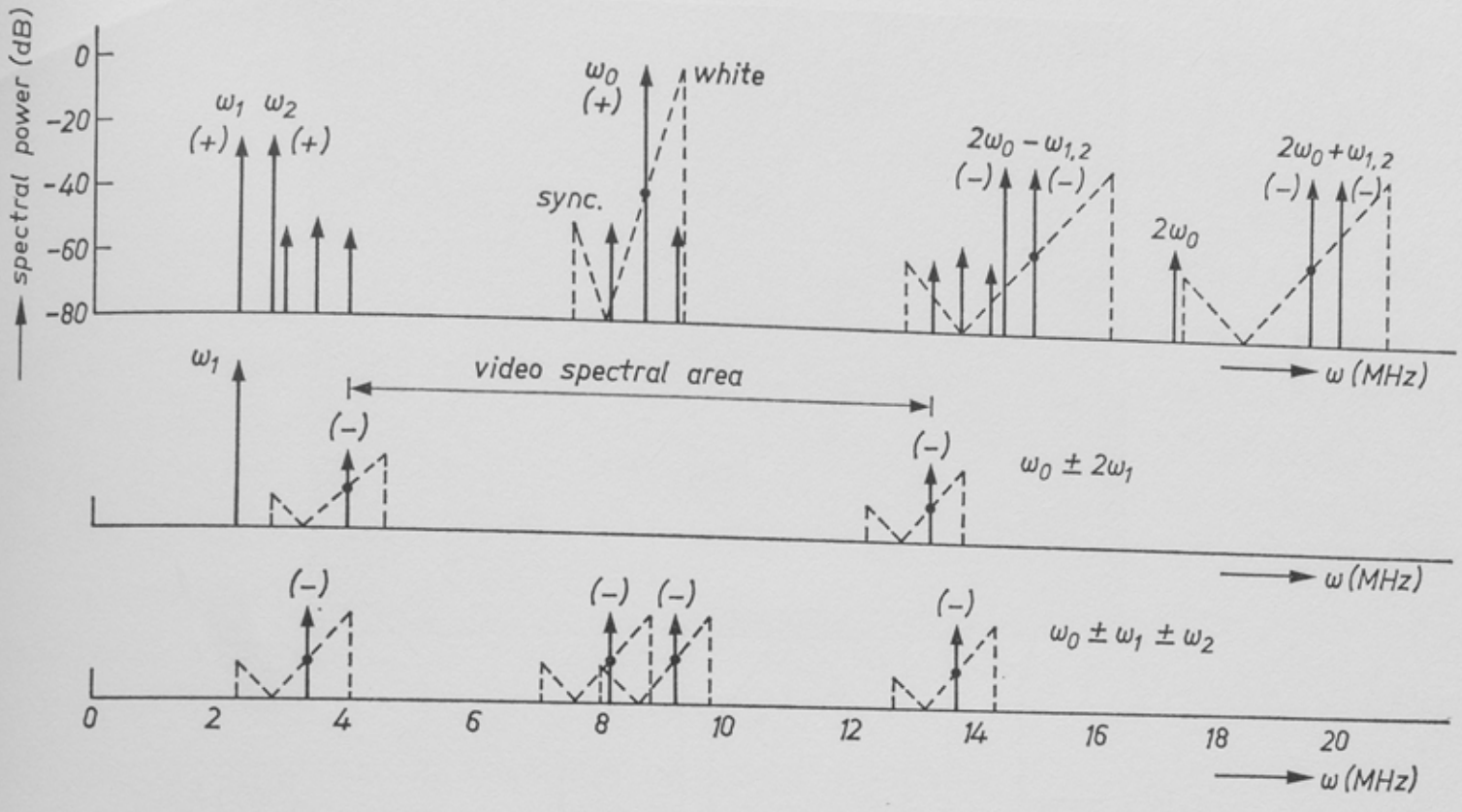

Fig. 11. Spectrum of the writing signal $y(t)$ in the absence of chrominance information. The relative movement on the frequency axis of the components $\omega_0 \pm 2\omega_1$ and $\omega_0 \pm \omega_1 \pm \omega_2$ is shown separately.

the video signal is indicated by the dashed lines. All arrows are related to a grey level of 50 %, giving an instantaneous carrier at 8.6 MHz.

We calculated the amplitudes with the aid of the formalism developed in sec. 2. For a symmetrical hard limiter with sinusoidal input-wave forms the amplitudes a_{lmn} of all the above mentioned components are given for $l + m + n$ = uneven by equation (12) with $x_a = 0$.

An experimental result is shown in fig. 12, where we have chosen slightly different sound carrier frequencies to facilitate visual interpretation of the components. We found

l,m,n	components	ampl. calc. (dB)	ampl. exp. (dB)	polarity
1,0,0	ω_0	0	0	(+)
0,1,0	ω_1, ω_2	−25.9	−26.5	(+)
1,2,0	$(\omega_0 \pm 2\omega_1), (\omega_0 \pm 2\omega_2)$	−56.0	−57	(−)
2,1,0	$(2\omega_0 \pm \omega_1), (2\omega_0 \pm \omega_2)$	−26.1	−26.5	(−)
1,1,1	$\omega_0 \pm \omega_1 \pm \omega_2$	−51.9	−52	(−)

Because of our initial choice of cosine-wave forms as inputs to the limiter, the output spectrum is real and all output components can be described as cosine functions with proper polarity, indicating the mutual phase relationships.

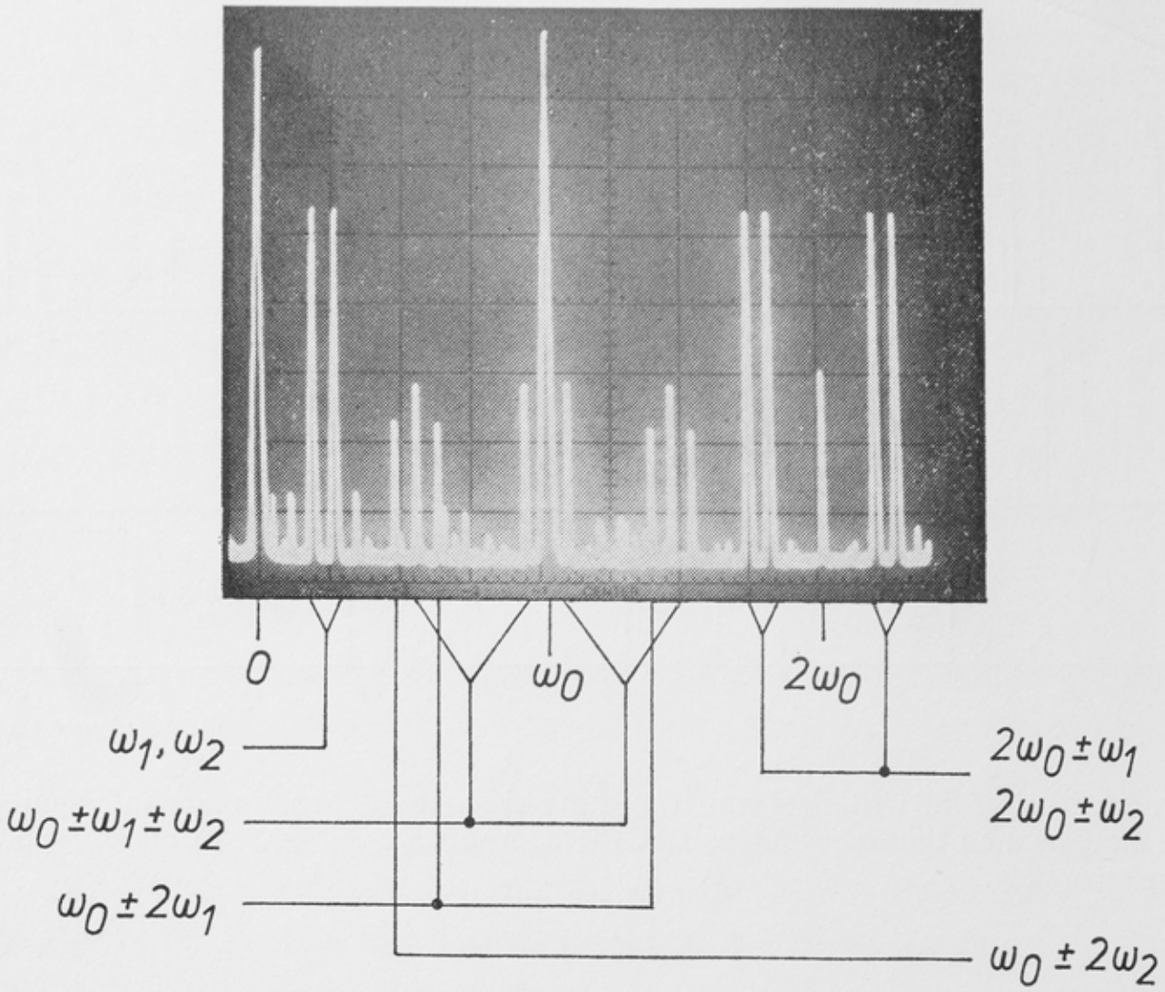

Fig. 12. Measured spectrum of the writing signal without video modulation. Vert.: 10 dB/div.; Hor.: 0–20 MHz, 2 MHz/div. Perfect symmetrical limiting. The subcarrier frequencies at ca 1.2 and 2.0 MHz are chosen for convenient visual identification.

From the polarity we see that the components $+a_{0,1,0} \cos \omega_1 t$ and $-a_{2,1,0} \cos (2\omega_0 - \omega_1)t$ can be regarded as the two first-order sidebands of the carrier ω_0, whose frequency is modulated with a signal $\cos (\omega_0 - \omega_1)t$. The movement on the frequency axis of the components $(\omega_0 \pm 2\omega_1)$, $(\omega_0 \pm 2\omega_2)$ and $(\omega_0 \pm \omega_1 \pm \omega_2)$ as function of the luminance level are indicated separately in fig. 11. All these components move synchronously with ω_0 and possible interference in the demodulated video signal will therefore always have a fixed frequency independent of the luminance level.

The two strongest components near the carrier are $\omega_0 \pm (\omega_2 - \omega_1)$ at distances of 0.5 MHz from ω_0. Ideally, both components behave as AM sidebands to the carrier. Making an unrealistic worst-case assumption that the upper sideband is erased, for example by filtering, leaving only the lower sideband and the main carier, we can calculate the resulting amplitude of the interference frequency (0.5 MHz). With a level of −52 dB in the spectrum and neglecting the de-emphasis, which is still small at this frequency, we would find the peak-to-peak value of the interference signal in the demodulated video at −53.6 dB with respect to the black-to-white amplitude (700 mV).

Until now we have only considered that group of components with $l + m + n =$ uneven, which is generated even in the absence of asymmetry.

When a small asymmetry is introduced the amplitudes of these components do not change very much, because of the cosine dependence on x_a in eq. (11). However, the introduction of asymmetry gives rise to a second group of components, which represents the intermodulation products of order $l + m + n =$ even, with amplitudes given by eq. (12). As discussed in secs 2 and 3, the influence of the asymmetry related to the writing and development steps can be formalized as a change in the offset parameter x_a. Thus, where we have asymmetry ($x_a \neq 0$), for example the components $\omega_0 \pm \omega_1$ and $\omega_0 \pm \omega_2$ are generated. At playback these components together with the FM-modulated main carrier are applied to the input of a FM demodulator having the required bandwidth for the video signal. The video spectral area at best comprises the main carrier and both first-order colour sidebands and ranges, in our case, from 4–13 MHz.

It is important to emphasize again that only when the amplitudes and phases of both components of each set of intermodulation products (i.e. $\omega_0 \pm \omega_1$) arrive unchanged at the input of the demodulator, will there be no generation of the unwanted frequency ω_1 in the demodulated video signal. In general these requirements are not met due to the amplitude versus frequency characteristic of the reading process. One could try, however, to compensate for this in designing a suitable equalizing network that restores an equal amplitude to both components without altering their phase relationships. Moreover, the equalizing has to be adaptable to the radius of the tracks.

In figure 13 the positions of the different components are shown for the case of an unmodulated main carrier ω_0 and one sound carrier ω_1. Further asymme-

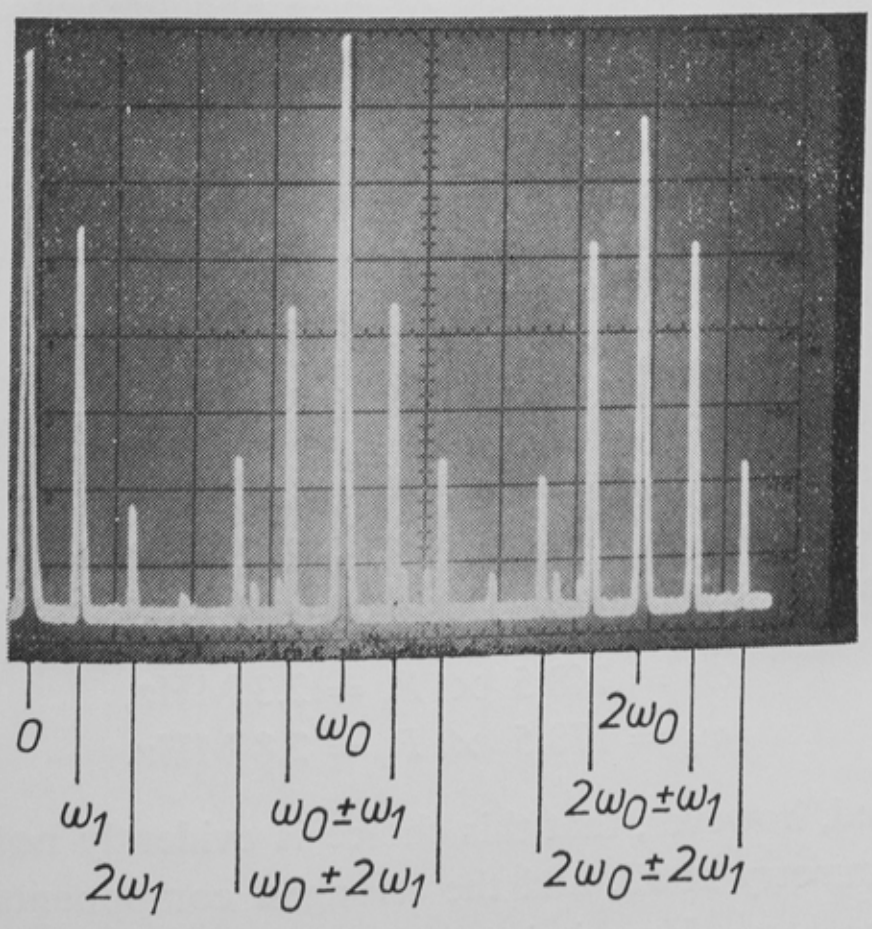

Fig. 13. Identical to fig. 12 except that only one sound carrier is shown and that a 20% asymmetric setting of the limiter level is used.

try components that can be observed, are $(2\omega_0 \pm 2\omega_1)$, and $2\omega_1$. Also the 2nd harmonic $2\omega_0$ has increased considerably. The amount of asymmetry introduced here is 20% (60/40 proportionality of the duty cycle related to a square-wave form) and corresponds to a value of the asymmetry parameter $x_a = 0.314$.

Figure 14 gives the measured spectrum for the same asymmetry but now with two subcarriers. From the second subcarrier the asymmetry components $(\omega_0 \pm \omega_2)$, $(2\omega_0 \pm 2\omega_2)$ and $2\omega_2$ are generated. Moreover, additional cross components are enhanced, also a function of asymmetry: $2\omega_0 \pm \omega_1 \pm \omega_2$ and $\omega_2 \pm \omega_1$.

The amplitudes a_{lmn} of the asymmetry components $(l + m + n = \text{even})$ were calculated from (11) with $x_a = 0.314$.
We found:

l,m,n	components	ampl. calc. (dB)	ampl. exp. (dB)	polarity
2,0,0	$2\omega_0$	−11.6	−12	(−)
0,2,0	$2\omega_1, 2\omega_2$	−66.0	−65/−67	(−)
1,1,0	$(\omega_0 \pm \omega_1), (\omega_0 \pm \omega_2)$	−34.0	−36	(−)
0,1,1	$\omega_2 \pm \omega_1$	−52.2	−50.5	(+)
2,2,0	$(2\omega_0 \pm 2\omega_1), (2\omega_0 \pm 2\omega_2)$	−59.9	−58	(+)
2,1,1	$2\omega_0 \pm \omega_1 \pm \omega_2$	−46.2	−53	(+)

Figure 15 summarizes all components of even and uneven order that are of interest within the video spectral area, allowing for 20% asymmetry. The strongest asymmetry components are $(\omega_0 \pm \omega_1)$ and $(\omega_0 \pm \omega_2)$ at −36 dB. If only the lower components $(\omega_0 - \omega_1)$ and $(\omega_0 - \omega_2)$ were present at the input of the demodulator, we would find interference frequencies in the demodulated video at 2.3 and 2.8 MHz with levels of −29 dB and −28 dB respectively, as a worst case taking the de-emphasis into account.

In order to further minimize the visibility of these interferences in the picture it is advantageous to use a frequency-offset compared to the line-scan frequency F_h for the mean values of the sound carrier frequencies ω_1 and ω_2. Selecting an odd half multiple of F_h for ω_1 and ω_2 will give the best visual cancelling:

$$\omega_1 = 148.5 \times F_h = 2.3 \text{ MHz},$$
$$\omega_2 = 178.5 \times F_h = 2.8 \text{ MHz}.$$

It should be noted, however, that this choice is evidently not optimal in case we have no asymmetry at all, and the strongest components in the spectrum become $\omega_0 \pm \omega_1 \pm \omega_2$. Here it is more advantageous to select respectively $a = \frac{1}{4}$ and $a = \frac{3}{4}$ line offset for the sound subcarriers. (E.g. $\omega_1 = 148.25\, F_h$

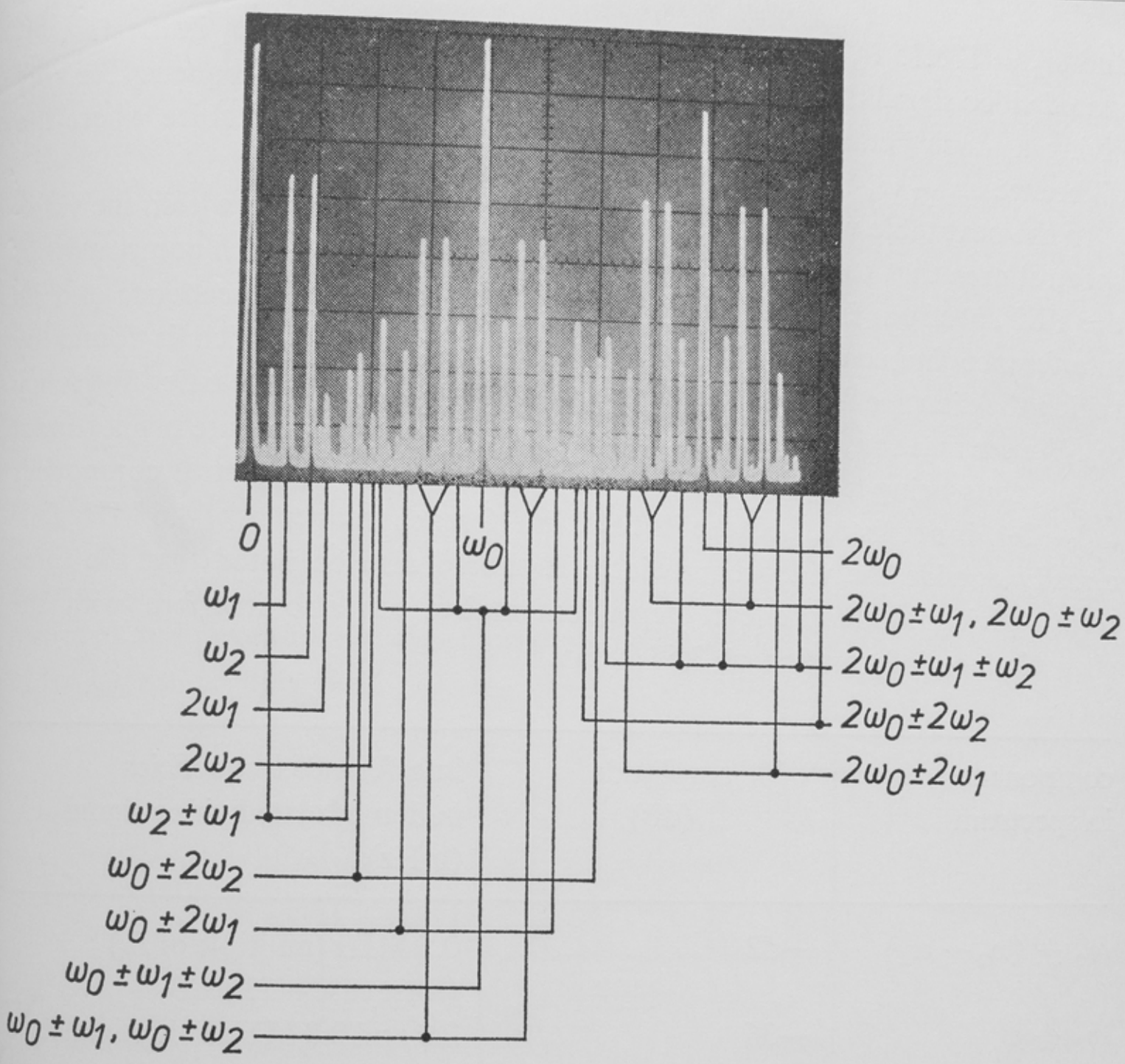

Fig. 14. Complete spectrum of a 20% asymmetrical writing signal $y(t)$ with two subcarriers. Main carrier unmodulated.

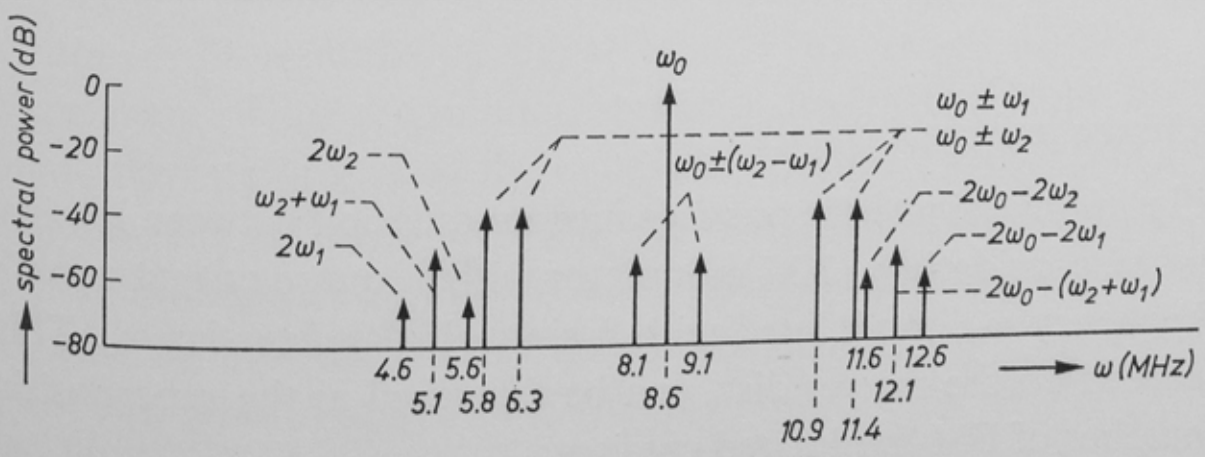

Fig. 15. Actual location of the sound intermodulation products within the video spectral area. The movements of the components relative to the carrier frequency can easily be found by varying ω_0. Sound carrier frequencies correspond to system choice: 2.3 and 2.8 MHz.

and $\omega_2 = 178.75\ F_h$). For the interference of frequency $\omega_2 - \omega_1$ in the demodulated video signal this choice results in a net half line offset at frequency $30.5\ F_h$, giving a much better visual cancelling than with the actual choice where the difference $\omega_2 - \omega_1$ is equal to a multiple of F_h.

In the next table we now summarize all spectral components within the video spectral area that can affect the demodulated video signal. Each component in the FM spectrum is listed with its amplitude, symmetry dependence and its interference frequency in the demodulated video signal, which is found by taking the distance from each component to the instantaneous carrier frequency ω_0. We see that some of the interferences have frequencies that are proportional to ω_0, thus being a function of the luminance level. The spectral component $\omega_0 - 2\omega_1$ is not listed, because its fixed interference frequency of 4.6 MHz falls already outside the video bandwidth. It should also be noted that the three terms, giving luminance-level dependent moiré, can also interfere with the chrominance information at 3.58 MHz.

component in spectrum	amplitude (dB)	interference frequencies in demodulated video signal (mHz)
$\omega_0 \pm (\omega_2 - \omega_1)$	−52	0.5 MHz (multiple of F_h) worst case −53.6 dB
$\omega_0 \pm \omega_1$	−36	2.3 and 2.8 MHz in luminance band, with half line offset
$\omega_0 \pm \omega_2$	(20% asym.)	
$2\omega_2$	−60	2.4–3.6 MHz luminance-level dependent moiré
$2\omega_0 - 2\omega_2$	−58 (20% asym.)	
$\omega_2 + \omega_1$	−50.5	2.2–4.1 MHz luminance-level dependent moiré
$2\omega_0 + (\omega_2 + \omega_1)$	−53 (20% asym.)	
$2\omega_1$	−60	3.4–4.6 MHz luminance-level dependent moiré
$2\omega_0 - 2\omega_1$	−58 (20% asym.)	

4.2. *Luminance and chrominance*

We will now investigate the possible intermodulation between luminance and chrominance, considering a FM modulator with a square output waveform and carrier frequency ω_0, modulated with a sinusoidal subcarrier ω_c. This signal, to be recorded on the master disc, can be described as the superposition of an infinite number of FM-modulated carriers:

$$\sum_{k=1}^{\infty} c_k \operatorname{Re} \{\exp [\mathrm{i}\,(k\omega_0 t + km \cos \omega_c t)]\},$$

where c_k are the Fourier coefficients of the unmodulated square-wave carrier signal and m is the modulation index.

From the discussion in sec. 3.1 we have seen that the simple approximation of our channel by an asymmetrical limiter followed by a linear filter with cut-off frequency ω_p is not valid for the case of an FM signal. The recording and reading processes, as formalized by eq. (14) and (15) respectively, both generate baseband signals at frequency ω_c. By the fact that the filtering of the reading operation is strongest, the amplitude of the baseband signal is mainly proportional to $2m\omega_c/\omega_p$ as indicated in sec. 3.2. This value is, however, of limited importance if we consider the possibility of obtaining longer or shorter pulses by controlling the intensity of the writing beam and the development time of the master. In that case eq. (14) does no longer hold and the mechanism is best described as the addition of pulses of fixed duration to each side of the original square-wave pulses. (See fig. 16.) This asymmetrical signal now represents the recorded and developed track signal that will be played back through the filter of the optical reading step.

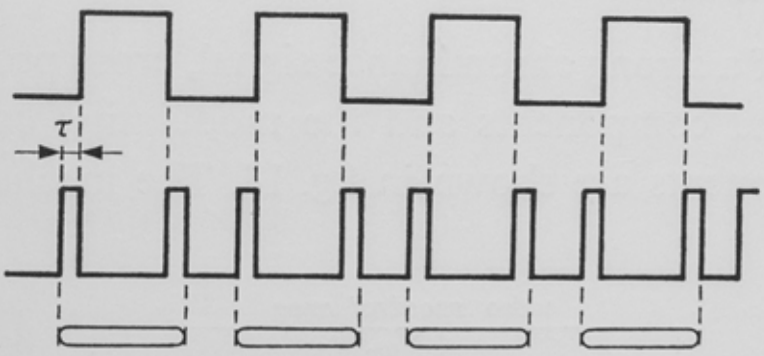

Fig. 16. Schematic representation of pit lengthening by fixed amounts. The asymmetrical duty cycle of the pits can be seen as the summation of a pulse train with constant pulses to the original symmetrical writing signal.

The spectrum of the asymmetrical signal can be separated into two parts: one of the original symmetrical FM wave and one of a pulse train at double frequency with fixed pulsewidth. The spectrum of the extra pulse train is indentical to that constructed in the well-known "pulse counter FM demodulation" technique [11]). Analysis of this spectrum shows that it contains not only the spectrum of the modulating signal around the second harmonic $2\omega_0$, but also the spectrum of the modulating signal ω_c itself (baseband). Here we will not estimate the amplitudes of the enhanced spectral components as they are rather unimportant for the following discussion and are a function of a number of varying technological parameters. More interesting are their positions on the frequency axis, as indicated for our system in fig. 17.

The most important requirement for the choice of the carrier frequency ω_0 is that the first-order lower chrominance sideband must not overlap with the chrominance baseband at ω_c. If so they would interfere heavily, giving variable moiré in the demodulated chrominance signal. Therefore the black-level fre-

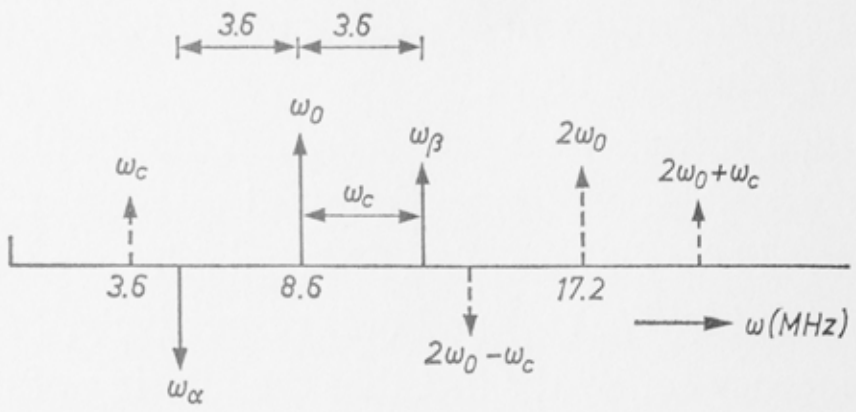

Fig. 17. Generation of the baseband component ω_c as a result of the asymmetry of the track structure as indicated in fig. 16. $\omega_\alpha = \omega_0 - \omega_c$; $\omega_\beta = \omega_0 + \omega_c$.

quency has been chosen at 8.0 MHz [4]), which guarantees a frequency distance $\geqslant$ 800 kHz between $\omega_0 - \omega_c$ and ω_c. Taking into account the bandwidth of the chrominance signals ($\pm$ 500 kHz), this 800 kHz separation constitutes a lower limit to circumvent annoying chrominance interference when allowing for an asymmetry up to 20%.

4.3. *Chrominance and sound*

In the presence of a strong chrominance signal, cross products are generated between some sound components and the modulating colour subcarrier ω_c. The relevant components are shown in fig. 18. The mechanism is most easily

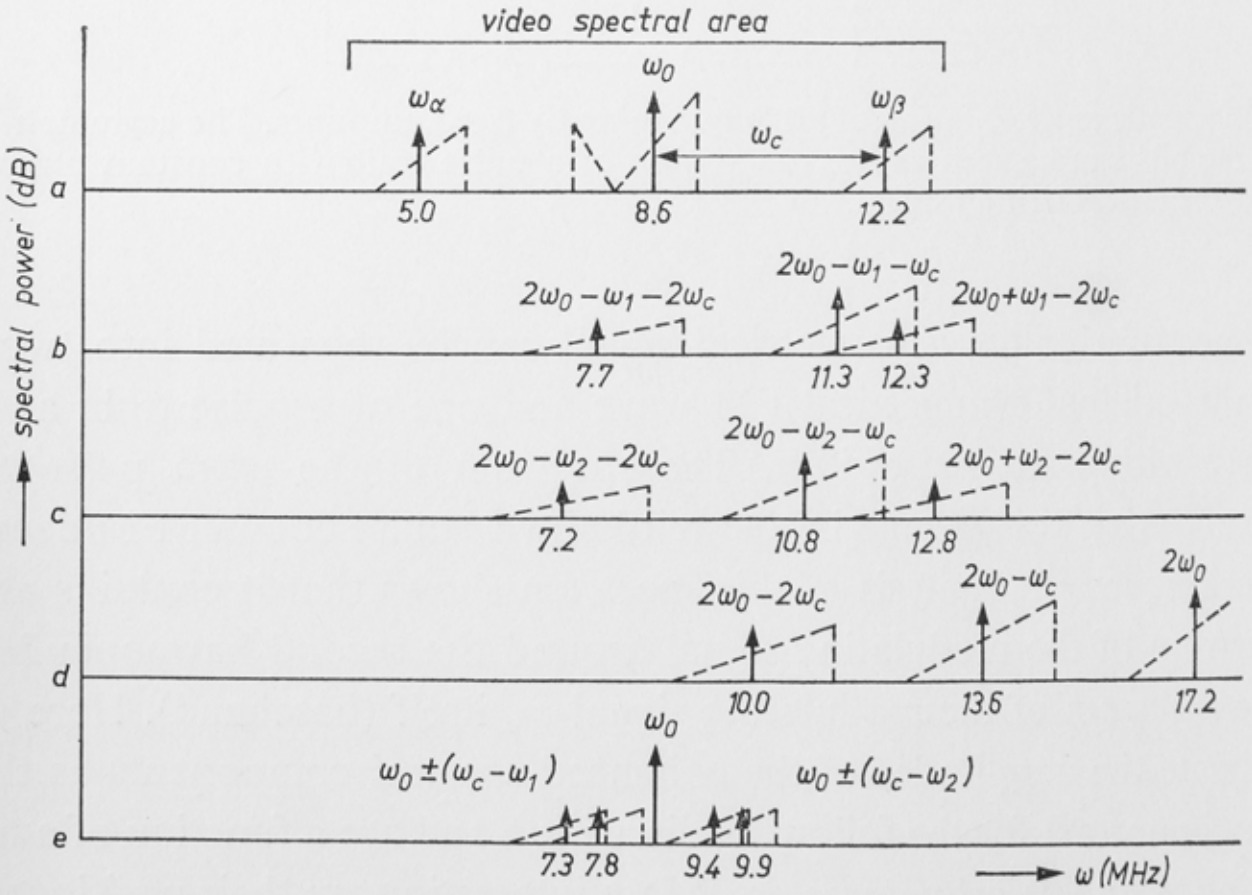

Fig. 18. Positions of the relevant intermodulation products between chrominance sidebands and the two sound carriers. Only the components on the two lower lines are generated by asymmetry. All components vanish in the absence of chrominance. The different lines of the figure show the following spectra: (*a*) spectrum of the colour-modulated video signal, (*b*) colour sidebands of $2\omega_0 \pm \omega_1$, (*c*) idem of $2\omega_0 \pm \omega_2$, (*d*) idem of $2\omega_0$, with 20% asymmetry, (*e*) idem of $\omega_0 \pm \omega_1$ and $\omega_0 \pm \omega_2$, also with 20% asymmetry. The frequencies $\omega_0 \pm \omega_c$ are denoted by ω_α and ω_β.

explained by looking first at the PWM spectrum of one sound carrier, as given for example by fig. 13. Taking the components $2\omega_0 \pm \omega_1$, we see that if ω_0 is FM-modulated with ω_c, the same modulation is induced on them with a modulation index that is twice as large by the fact that $2\omega_0 - \omega_1$ has double the frequency deviation. Considering therefore $2\omega_0 \pm \omega_1$ as FM carriers with modulating frequency ω_c, we find for example $2\omega_0 \pm \omega_1 \pm \omega_c$ as first-order sidebands (see fig. 18*b*).

The strength of these components can be calculated directly as $a_{2,1,0}\, J_1(2m)$, where $m = \Delta\omega/\omega_c$ and $a_{2,1,0}$ is the amplitude of the $2\omega_0 \pm \omega_1$ components with respect to the main carrier from eq. (12). As the chrominance amplitude is directly proportional to $\Delta\omega$ these components all vanish in the absence of colour information. For a full-colour signal (75% saturated red or cyanic, $m = 0.32$) the amplitude is equal to −36 dB. The same applies to the second sound carrier ω_2 giving $2\omega_0 \pm \omega_2 \pm \omega_c$ at a level of −36 dB, indicated in fig. 18c. Second-order sidebands are generated at frequencies $2\omega_0 \pm \omega_1 \pm 2\omega_c$ and $2\omega_0 \pm \omega_2 \pm 2\omega_c$ at a level of −52 dB. All these components will be generated even in the absence of asymmetry ($x_a = 0$), but vary in strength with the colour saturation. Their effect in the demodulated video signal is moiré of variable frequency, as can be seen by observing the distance from the main carrier ω_0. The moiré frequencies are thus a function of the luminance level, and listed below for the black-to-white range.

components in spectrum	amplitude (dB) (for 75% red)	interference frequencies in demodulated video signal (MHz)
$2\omega_0 - \omega_1 - \omega_c$	−36	2.1 – 3.3
$2\omega_0 - \omega_2 - \omega_c$	−36	1.6 – 2.8
$2\omega_0 - \omega_2 - 2\omega_c$	−52	0.3 – 1.5
$2\omega_0 - \omega_2 - 2\omega_c$	−52	0.8 – 2.0
$2\omega_0 + \omega_1 - 2\omega_c$	−52	3.1 – 4.3
$2\omega_0 + \omega_2 - 2\omega_c$	−52	3.6 – 4.8

The most harmful components are $2\omega_0 - \omega_{1,2} - \omega_c$ at −36 dB. With this value the amplitude of the interference signal in the demodulated video of for example 2.5 MHz will be as high as −29.5 dB.

Where an asymmetry of 20% is encountered the possible colour sidebands of $2\omega_0$ and of its associated asymmetry components $\omega_0 \pm \omega_1$, $\omega_0 \pm \omega_2$ must be investigated. (see for example fig. 14). Having $2\omega_0$ at a level of −12 dB, the first-order sidebands $2\omega_0 \pm \omega_c$ will be at −22 dB and the second-order sidebands $2\omega_0 \pm 2\omega_c$ at −38 dB. Only the last-named will penetrate in the video spectral area, as can be seen from fig. 18*d*.

Of all the possible first-order sidebands around $\omega_0 \pm \omega_1$ and $\omega_0 \pm \omega_2$ only the components $\omega_0 \pm (\omega_c - \omega_1)$ and $\omega_0 \pm (\omega_c - \omega_2)$ have frequencies within the video spectral area (fig. 18*e*). Their level in the FM spectrum is at −52 dB for 20% asymmetry and 75% saturated red or cyanic colours. After demodulation these components give rise to fixed intermodulation frequencies of 0.8 and 1.3 MHz, both being an exact multiple of the line-scan frequency, due to the fact that ω_c, ω_1 and ω_2 all have half line offset (see sec. 4.1). Summarizing the asymmetry-dependent components and their possible interference frequencies in the demodulated video we have:

component in spectrum	amplitude (dB) (for 70% red)	interference frequencies in demodulated video (MHz)
$2\omega_0 - 2\omega_c$	−38	0.8 – 2.0
$\omega_0 \pm (\omega_c - \omega_1)$	−52	1.3 } independent of
$\omega_0 \pm (\omega_c - \omega_2)$	−52	0.8 } luminance level

The most disturbing component $2\omega_0 - 2\omega_c$ will give rise to an interference amplitude in the video of −35.5 dB at a frequency of 1.4 MHz corresponding to a 50% grey level of the luminance signal.

5. Conclusions

The intermodulation products can be separated into two groups: one that is independent of asymmetry of the channel and gives rise to components that will never vanish, and a second group with components that are only generated in the presence of asymmetry. As we will have to allow for some asymmetry (up to 20%) it is necessary to consider all components when selecting carrier frequencies and relative amplitudes.

For the luminance–chrominance intermodulation the most important effect is the generation of a baseband chrominance signal in the FM spectrum. The wish to circumvent possible interference from this baseband into the first-order chrominance sideband, requires a carrier frequency higher than 8.0 MHz.

The interference of the sound subcarriers is attenuated by different measures. Firstly the subcarrier frequencies are chosen such that their second-harmonic frequencies $2\omega_1$ and $2\omega_2$ and also their mutual sum frequency $\omega_1 + \omega_2$ fall outside the video bandwidth. Secondly the frequency offset of the sound carriers with respect to the line-scan frequency F_h of the television system is chosen such that the asymmetry components $\omega_0 \pm \omega_1$ and $\omega_0 \pm \omega_2$ in the FM spectrum will yield interference frequencies after demodulation that possess a half line offset, thus making an optimum use of the visual cancelling of the eye from line to line on the picture screen. We are always left with the difference component $\omega_2 - \omega_1$ (500 kHz) in the video signal, having no offset and thus being

maximally visible, however, its level is relatively low (< -53.6 dB). In a channel without asymmetry the signal-to-moiré ratio due to the presence of both pulse-width-modulated sound carriers alone is greater than 45 dB.

A characteristic for the chrominance–sound intermodulation is that the strongest components, being formed by the first-order colour sidebands of the "subcarriers" $2\omega_0 \pm \omega_1$ and $2\omega_0 \pm \omega_2$, are independent of asymmetry, so that nothing can be done to neutralize these. However, their amplitude is a function of the colour saturation and therefore the effects will only be visible in high saturated areas of the picture. (-30 dB for a 75% saturated red or cyanic.

Thus, the analysis of intermodulation products in the VLP system shows that, by a judicious choice of the frequencies of the luminance, colour and sound components of the recorded signal, it is possible to obtain T.V. pictures of good quality.

Philips Research Laboratories *Eindhoven, Oktober 1977*

Appendix

We calculate the intermodulation products of a memoryless limiter with characteristic $y = f(x)$ (4) and an input given by the sum of two periodic signals. The theory can be generalized straightforwardly to the case of N periodic signals. Let the input signal be given by

$$x(t) = x_a + x_1(t) + x_2(t), \tag{A1}$$

where x_a is a constant bias and x_1 and x_2 are even, periodic functions of arguments $\varphi_1(t)$ and $\varphi_2(t)$ (see eq. (6) of sec. 2), $x_j(t) = \tilde{x}_j[\varphi_j(t)]$.

The output signal y can be written as a double Fourier series in φ_1 and φ_2:

$$y = \sum_{m=-\infty}^{\infty} \sum_{n=-\infty}^{\infty} a_{mn} \exp\,[\mathrm{i}\,(m\varphi_1 + n\varphi_2)]. \tag{A2}$$

The coefficients a_{mn} are real and even in the indices m and n. From (A2) we have

$$a_{mn} = \frac{1}{(2\pi)^2} \int_{-\pi}^{\pi} \int_{-\pi}^{\pi} f(x_a + \tilde{x}_1(\varphi_1) + \tilde{x}_2(\varphi_2)) \exp\,[-\mathrm{i}\,(m\varphi_1 + n\varphi_2)]\,\mathrm{d}\varphi_1\,\mathrm{d}\varphi_2. \tag{A3}$$

We now assume that $f(x)$ can be written as a Fourier integral

$$f(x) = \frac{1}{2\pi} \int_{-\infty}^{\infty} F(s) \exp\,(\mathrm{i}xs)\,\mathrm{d}s. \tag{A4}$$

In the classical theory of the Fourier transforms [6]) $F(s)$ can be determined only for those functions $f(x)$ that are absolutely integrable over the interval

$-\infty < x < \infty$. With the help of the theory of generalized functions we can also define the Fourier transform of functions such as x^k and the Heaviside step function that do not fulfil this condition. This is important because functions like these often occur as idealized forms of limiter characteristics. We define functions $g_{jl}(s)$ by

$$g_{jl}(s) = \frac{1}{2\pi} \int_{-\pi}^{\pi} \exp\left[is\tilde{x}_j(\varphi_j) - il\varphi_j\right] \mathrm{d}\varphi_j. \tag{A5}$$

Inserting this, with (A4), in (A3) we obtain

$$a_{mn} = \frac{1}{2\pi} \int_{-\infty}^{\infty} F(s) \exp\left(ix_a s\right) g_{1m}(s)\, g_{2n}(s)\, \mathrm{d}s. \tag{A6}$$

This formula is a generalization of formula (6) in the paper by Bennett and Rice [5]). The functions $g_{jl}(s)$ can be easily found for two cases: sinusoidal and piecewise linear signals. We give $F(s)$ for some important cases. For a limiter characteristic of the form

$$y = x^k \, sgn\,(x), \tag{A7}$$

where k is a positive integer and where the function $sgn(x)$ is defined by

$$\begin{aligned} &= 1 && x > 0 \\ sgn(x) &= 0 && x = 0 \\ &= -1 && x < 0 \end{aligned} \tag{A8}$$

the Fourier transform is given by (7)

$$F(s) = 2\,k!\,(is)^{-k-1}, \tag{A9}$$

where s^{-k} is to be considered as a generalized function. Inserting this in (A6), using the appropriate definition of s^{-k} [7]), we obtain

$$a_{mn} = \frac{1}{\pi i^{k+1}} \int_{-\infty}^{\infty} \frac{1}{s} \frac{\mathrm{d}^k}{\mathrm{d}s^k} \left[\exp\left(ix_a s\right) g_{1m}(s)\, g_{2n}(s)\right] \mathrm{d}s. \tag{A10}$$

For a limiter with the characteristic

$$y = x^k, \tag{A11}$$

where k is a positive integer we obtain from ref. 7

$$F(s) = 2\pi i^k \, \delta^{(k)}(s), \tag{A12}$$

where $\delta^{(k)}(s)$ is the kth derivative of the Dirac delta function and

$$a_{mn} = \mathrm{i}^k \left\{ \frac{\mathrm{d}^k}{\mathrm{d}s^k} \left[\exp(\mathrm{i}x_a s)\, g_{1m}(s)\, g_{2n}(s) \right] \right\}_{s=0}. \tag{A13}$$

When the nonlinearity is of the form

$$y = x^k H(x), \tag{A14}$$

where the Heaviside step function is defined by

$$H(x) = \tfrac{1}{2}(1 + sgn(x)) \tag{A15}$$

the Fourier coefficients can be found by averaging the results of (A13) and (A10). We then find expressions equivalent to those deduced by Bennett and Rice [5]). Our expressions have the advantage that singularities at $s = 0$ are avoided by the use of generalized functions. By superposing nonlinearities of the types given by (A7), (A11) and (A14) we can approximate many of the limiter characteristics that occur in practice.

We have not specified the form of the signals $\tilde{x}_i(\varphi_i)$; the expressions (A13) and (A10) are therefore valid for all periodic, bounded input signals.

REFERENCES

1) B. A. J. Jacobs, Laser beam recording of video master discs, to be published in Applied Optics.
2) G. Bouwhuis and J. J. M. Braat, Video disc player optics, to be published in Applied Optics.
3) M. R. de Haan, J. Royal T.V. Soc., **16**, 187, 1976.
4) P. W. Bögels, IEEE Trans. on Consumer Electronics **CE22**, 309, 1976.
5) W. R. Bennett and S. O. Rice, Phil. Mag. **18**, 422, 1934.
6) A. Papoulis, The Fourier integral and its applications, McGraw-Hill, New York, 1962.
7) M. J. Lighthill, An introduction to Fourier analysis and generalized functions, Cambridge Univ. Press, New York, 1959.
8) M. Abramowitz and I. Stegun, Handbook of Mathematical Functions, 5th ed., Natl Bur. Stand., Washington, 1968.
9) C. H. F. Velzel, Laser beam reading of video discs, to be published in Applied Optics.
10) A. Bruce Carlson, Communication systems, McGraw-Hill, New York, 1968, chapter 6.
11) K.K. Clark and D.T. Hess, Communication circuits, Addison–Wesley, Reading, Mass., 1971, chapter 12.